Creep Deformation Behavior of Heating Filaments in High Temperature Applications

Bernhard Valentini[1]
[1]Plansee SE, Innovation Services
*Corresponding author: Bernhard Valentini, Metallwerk-Plansee-Straße 71, 6600 Reutte, Austria, bernhard.valentini@plansee.com

Abstract: Resistive heating filaments used in high temperature applications at 2000°C and above are often made of refractory metals. The lifetime of such filaments is mainly limited by creep deformations which can in the worst case lead to a short circuit between filaments and other furnace components. With the aid of COMSOL Multiphysics the time-dependent creep deformation behavior of a heater assembly with different shapes and arrangements of heating filaments is studied. In the numerical computations thermally induced stresses as well as electromagnetically induced Lorentz forces are considered. The creep deformation behavior is accounted for by a temperature and stress dependent creep model for isotropic metals under secondary creep.

Keywords: heating filament, high temperature creep, Lorentz force.

1. Introduction

In high temperature applications, e.g., in furnaces for sintering refractory metals or growing single crystals, resistive heating filaments made of refractory metals as tungsten or molybdenum are widely-used. At temperatures which are usually above 2000°C the heating filaments are exposed to stresses resulting from mechanical constraints and electromagnetically induced Lorentz forces. The lifetime of such filaments is often limited by creep deformations which can in the worst case lead to a short circuit between neighboring filaments or filaments and other furnace components, respectively. To this end predicting the time-dependent creep deformation behavior of heating filaments is an important part already during the development of new heaters.
With the aid of COMSOL Multiphysics the electromagnetically induced Lorentz forces are computed for different shapes and arrangements of heating filaments. Subsequently, the Lorentz forces are used in mechanical analyses to predict the stresses and the creep deformation of the heating filaments. The creep deformation behavior is accounted for by a creep model for refractory metals presented in [1].

2. Numerical model

2.1 Geometry

The investigated heater assembly consists of two fixed half rings representing the anode and cathode at the top, a short circuit ring at the bottom and a series of heating filaments in between. In Figure 1 the geometry of the heating filaments and the short circuit ring without the anode and cathode is shown for two setups. The N = {4, 8, 12, 16} heating filaments are made of tungsten, have a length of 700 mm and are arranged in a circular pattern. The thickness of all sheets is defined as 1 mm and their center plane is located at a cylinder with a diameter of 361 mm. The central angle α of the filaments is computed as

$$\alpha = \frac{360}{\mathrm{N}}(1-\beta) \qquad (1)$$

with β = 0.2 denoting the whitespace factor between the filaments. All heating filaments are connected to each other by a short circuit ring at the bottom. This tungsten ring has a thickness of 6 mm and a height of 20 mm. At the top one half of the heating filaments is connected to a massive copper half ring representing the anode and the remaining filaments are connected to a massive copper half ring representing the cathode. Since the structural stiffness of both copper half rings is high compared to those of the heating filaments and the short circuit ring, respectively, the copper rings are not modelled explicitly. However, their stiffness is considered by respective boundary conditions at the top of the heating filaments. Due to the twofold plane symmetry of the problem under consideration only one quarter of the heater assembly with respective boundary conditions is accounted for in the numerical model.

To avoid the computationally very expensive 3D evaluation of the electromagnetic induced Lorentz forces, the numerical model is split in two components: The magnetic field and the Lorentz forces are computed in a 2D-component which represents a plane orthogonal to the axis of the heater assembly at two-thirds of the height of the heating filaments. Hence, in the 2D-component only the cross section of the heating filaments and the surrounding atmosphere are considered (see Figure 2).

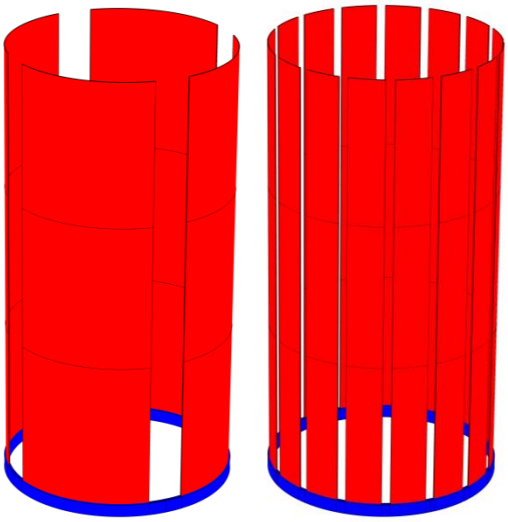

Figure 1. Geometry of the heater assembly with 4 filaments (left) and 16 filaments (right): heating filaments (red) and short circuit ring (blue).

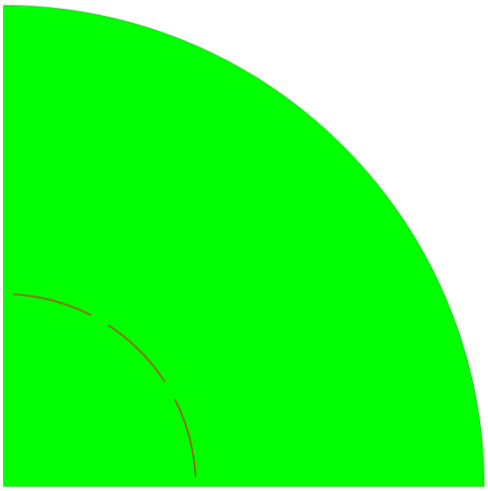

Figure 2. Geometry of one quarter of the heater assembly with 12 filaments used in the 2D-component: heating filaments (red) and surrounding atmosphere (green).

The mechanical behavior is computed with the aid of a 3D-component considering the heating filaments and the short circuit ring (see Figure 3) and the Lorentz forces computed in the 2D-component.

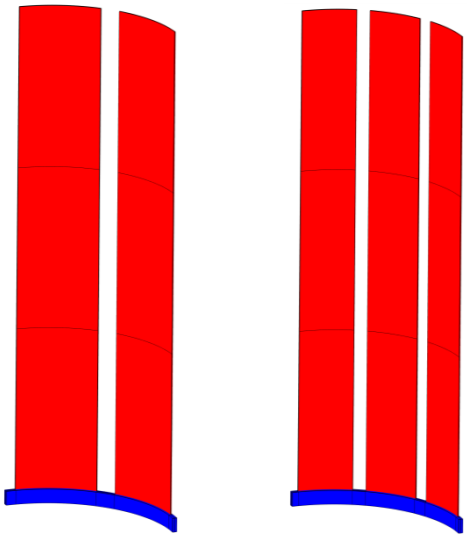

Figure 3. Geometry of one quarter of the heater assembly with 8 filaments (left) and 12 filaments (right) used in the 3D-component: heating filaments (red) and short circuit ring (blue).

2.2 Electromagnetic loading and boundary conditions

The 2D-component is loaded by an external electrical current density j directed orthogonal to the modelled plane, i.e. in (upward) axial direction of the heating filaments. The current density is ramped up from zero to a maximum current density j_{max} = 9.45 A/mm² in half a day, kept constant for eight days and then ramped down to zero in half a day. I.e., the assumed heating process cycle takes nine days. In the model the assumption is made that the electrical current in the heating filaments in the upper half space is directing out of the modelling plane and in the lower half space in the modelling plane. Hence, as boundary conditions the lower and circumferential edge of the domain representing the gas are magnetic insulators and the left edge is defined as a prefect magnetic conductor.

A general extrusion coupling is used to map the thermally induced deformations computed in the 3D-component to a *Deformed Geometry* feature in the 2D-component. Hence, the magnetic field

and the Lorentz forces are computed in the deformed configuration.

2.3 Structural loading and boundary conditions

For the short circuit ring at both planes of symmetry the displacement degrees of freedom orthogonal to the respective plane of symmetry are constrained. Additionally, at the top of the heating filaments the displacement degrees of freedom are constraint in all directions because of the high structural stiffness of the anode and cathode.
The dead load of all parts is considered in downward direction. At the beginning of the computation the whole heater assembly is assumed to be at room temperature. In the short circuit ring and the lower two-thirds of the heating filaments the temperature θ_{lower} is ramped up from room temperature to 2250°C in half a day, kept constant for eight days and then ramped down to room temperature in half a day. As a result of the intensely cooled anode and cathode the temperature in the upper third θ_{upper} is assumed as a linear function between room temperature at top and θ_{lower} at two-thirds of the height of the heating filaments (see Figure 4).

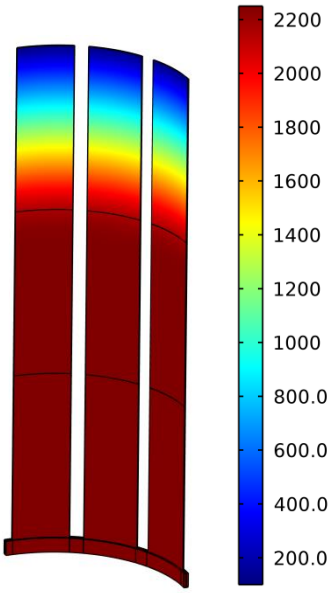

Figure 4. Temperature distribution [°C] of the heater assembly with 12 filaments used in the 3D-component after half a day.

A general extrusion coupling is used to map the electromagnetically induced Lorentz forces computed in the 2D-component to the 3D-component. Here the rough assumption is made that the Lorentz forces are constant along the height of the heating filaments. Furthermore, the Lorentz forces are applied as a body force only at the heating filaments.

2.4 Constitutive model

A temperature-dependent linear elastic-viscoplastic constitutive model for isotropic metals is used in the structural mechanics part of the model. Only the rate-dependent part of the viscoplastic material model is accounted for in the numerical model. It is described by the creep model presented in [1] which is implemented in COMSOL Multiphysics as a deviatoric creep model in the *Creep* subnode. The implemented creep law is able to describe the temperature and stress dependent mechanical behavior of isotropic metals under secondary creep (steady-state creep) taking into account dislocation creep (power law creep) as well as diffusion creep and/or grain boundary sliding.

2.5 Finite element mesh

The finite element mesh of the 2D-component and the 3D-component, respectively, is discretized by elements with quadratic order. In the 2D component quadrilateral elements are used for discretizing the domain representing the cross section of the heating filaments and triangular elements are used for the atmosphere surrounding the filaments. Boundary mesh layers are generated all around the heating filaments to enhance the quality of the finite element mesh. Hexahedral elements are used for discretizing the 3D-component. The layout of the mesh used for the cross section of the heating filaments in the 2D-component and the 3D-component is the same to avoid problems with the general extrusion couplings. For each of the four variants the number of degrees of freedom is about two million, primarily as a result of the seven degrees of freedom of the creep strain tensor at each node.

4. Results

4.1 Electromagnetic part

Figure 5 shows the predicted magnetic flux density norm and the Lorentz forces in radial direction of the heater assembly with 12 filaments after half a day (at maximum current density). The highest magnetic flux density is located at the short edge of the filament next to the plane of symmetry at the bottom. The plotted vectors of the radial component of the Lorentz forces are already integrated over the thickness of the heating filaments. As can be seen the radial component of the Lorentz forces are increasing with increasing distance from the plane of symmetry at the bottom and are not constant within each heating filament.

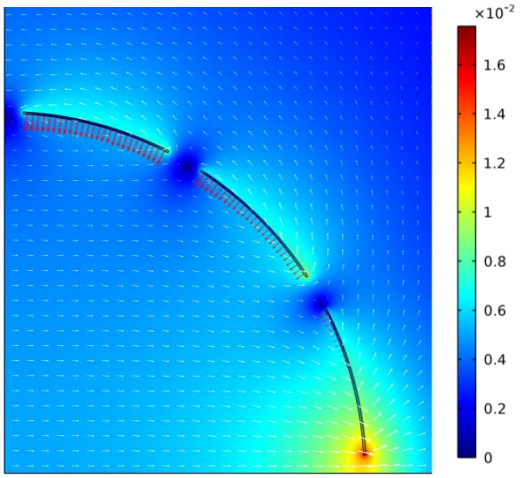

Figure 5. Magnetic flux density norm [T] (contour and white arrows) and radial component of the Lorentz forces (red arrows) of the heater assembly with 12 filaments after half a day.

For all variants in Figure 6 the radial component of the Lorentz forces – again already integrated over the thickness of the heating filaments – is plotted over the angle in counterclockwise direction starting at the plane of symmetry at the bottom. The gradient of the Lorentz forces along the arc length and the magnitude of the Lorentz forces is almost the same for all variants. However, the gradient along the arc length within each filament becomes more nonlinear with increasing number of filaments. The radial component of the Lorentz forces is always directed towards the center of the heater assembly. Hence, a deformation of the heating filaments towards the center is expected as a result of the Lorentz forces.

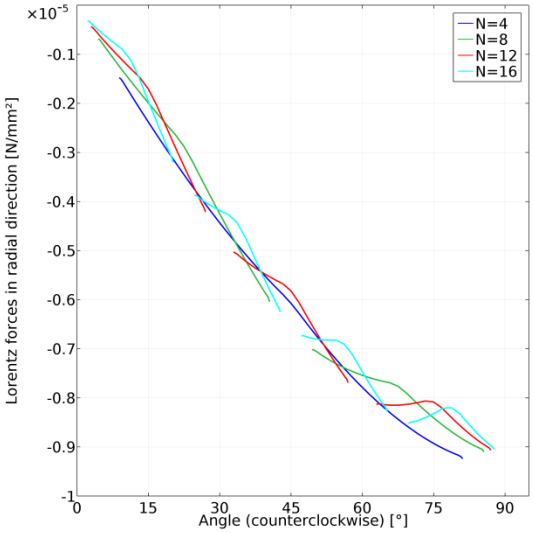

Figure 6. Radial component of the Lorentz forces over the angle in counterclockwise direction of all investigated heating assemblies after half a day.

4.2 Structural part

At the end of the process cycle (after nine days) the heating assembly is deformed due to the thermally induced stresses and the electromagnetically induced Lorentz forces acting on the heating filaments. In Figures 7 and 8 the radial displacements are plotted for all variants at the end of the computation. Note that the colored range of the displacements shown in Figure 7 is different to Figure 8. All variants have in common that the shape of the short circuit ring does not change because of its high bending stiffness compared to the heating filaments with respect to the loading situation. In the variant with four heating filaments the largest deformations are located at the vertical edges in the upper part of the heating filaments. The central region of the heating filaments is almost undeformed over the whole height. The displacements at the vertical edges of the heater assembly with eight filaments are not such pronounced as for the variant with four filaments. The minimum displacement in radial direction is about 40 % smaller than those of the variant with N = 4. As can be seen in Figure 8 the variants with 12 and 16 heating filaments, respectively, show larger deformations than the

two variants before. Furthermore, the radial displacements become almost constant along the arc length of each filament with increasing number of filaments. This is a result of the decreasing bending stiffness around the circumferential direction with decreasing arc length of the filaments. Since the Lorentz forces increase with increasing distance to the plane of symmetry (on the right-hand side) the influence of the Lorentz forces to the total deformations can be derived by the similarity of the deformation pattern of all heating filaments. While the heating filaments of the variants with N = 4 and 8 have an almost similar deformation pattern, respectively, in the variants with more filaments larger deformations are predicted in the filaments farthest from the plane of symmetry (on the right-hand side). As can be seen in Figure 9 neglecting the Lorentz forces for the variants with N = 12 and 16 leads to a uniform deformation patter of all heating filaments, respectively, and in addition to significantly smaller displacements. Hence, neglecting the Lorentz forces in the numerical computations for these two variants would lead to an underestimation of the creep deformations.

5. Conclusions

The comparative study of a heater assembly for high temperature applications shows that depending on the arrangement and geometry of the heating filaments creep deformations are not only a result of thermally induced stresses but also a result of electromagnetically induced Lorentz forces acting on the heating filaments. For the presented heater assembly with N = {4, 8, 12, 16} heating filaments Lorentz force induced creep deformations cannot be neglected in cases with more than eight filaments.

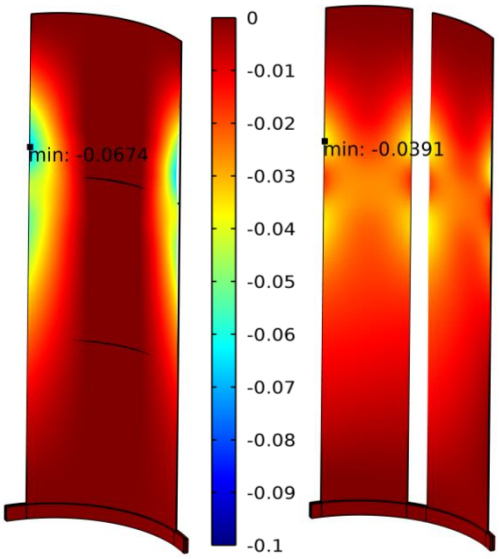

Figure 7. Radial displacements [mm] of the heater assembly with 4 filaments (left) and 8 filaments (right) at the end of the process cycle after nine days: deformations 100 fold magnified.

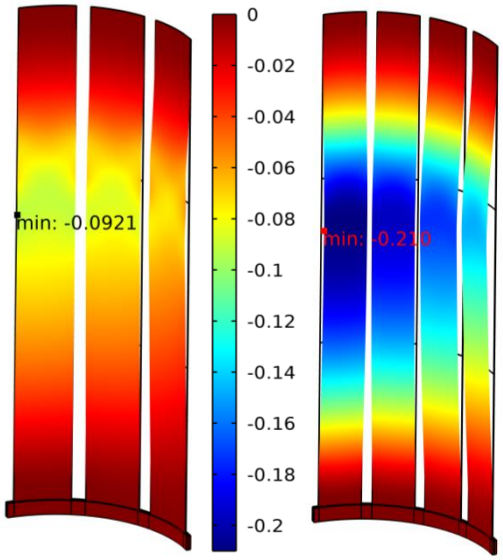

Figure 8. Radial displacements [mm] of the heater assembly with 12 filaments (left) and 16 filaments (right) at the end of the process cycle after nine days: deformations 100 fold magnified.

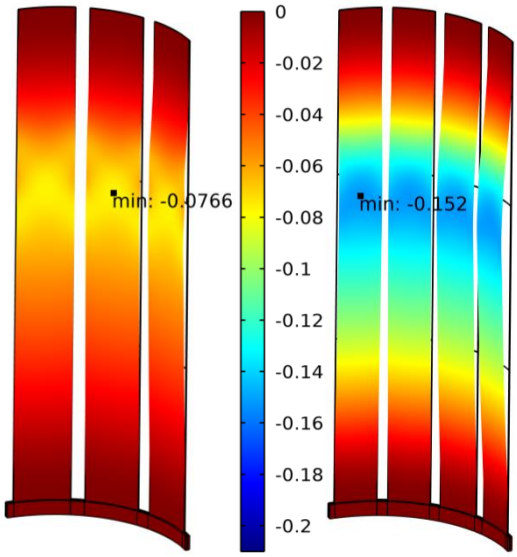

Figure 9. Radial displacements [mm] of the heater assembly with 12 filaments (left) and 16 filaments (right) without considering Lorentz forces at the end of the process cycle after nine days: deformations 100 fold magnified.

6. References

1. Valentini, B.; Leuprecht, C.; Plankensteiner, A.; Sigl L.S., Finite element analysis of the high-temperature creep deformation of a TZM heavy duty charge carrier, *International Journal of Refractory Metals and Hard Materials*, in press (2015)